Journal of Helminthology, page 1 of 14
doi:10.1017/S0022149X14000947

A new stem nematode, *Ditylenchus oncogenus* n. sp. (Nematoda: Tylenchida), parasitizing sowthistle from Adriatic coast dunes in southern Italy

N. Vovlas[1], A. Troccoli[1], J.E. Palomares-Rius[2], F. De Luca[1], C. Cantalapiedra-Navarrete[2], G. Liébanas[3], B.B. Landa[2], S.A. Subbotin[4,5] and P. Castillo[2]*

[1]Istituto per la Protezione Sostenibile delle Piante (IPSP), Consiglio Nazionale delle Ricerche (CNR), UOS di Bari, Via G. Amendola 122/D, 70126 Bari, Italy: [2]Instituto de Agricultura Sostenible (IAS), Consejo Superior de Investigaciones Científicas (CSIC), Apdo. 4084, 14080 Córdoba, Campus de Excelencia Internacional Agroalimentario, ceiA3, Spain: [3]Departamento de Biología Animal, Vegetal y Ecología, Universidad de Jaén, Campus 'Las Lagunillas' s/n, Edificio B3, 23071 Jaén, Spain: [4]Plant Pest Diagnostics Center (PPDC), California Department of Food and Agriculture, 3294 Meadowview Road, Sacramento, CA 95832-1448, USA: [5]Center of Parasitology of A.N. Severtsov Institute of Ecology and Evolution of the Russian Academy of Sciences, Leninskii Prospect 33, Moscow, 117071, Russia

(Received 28 June 2014; Accepted 22 December 2014)

Abstract

Morphological and molecular analyses of a stem nematode causing a severe disease on infected sowthistle (*Sonchus bulbosus*) plants, involving the formation of gall-like structures on infected leaves and stems, have led to the description of a new species named *Ditylenchus oncogenus* n. sp. Morphologically, the new species is characterized by a medium to large body size (all adults more than 1 mm in length); a delicate stylet (9.0–11.0 μm long) with minute, rounded knobs; a long post-vulval uterine sac (*c*. 65% of the vulva–anus distance); six incisures at the lateral fields and characteristic *D. destructor*-pattern of spicules (with pronounced ventral tumulus and anteriorly pointed, less sclerotized, cuticle parts present within the lamina). The results of molecular analysis of rRNA gene sequences, including the D2–D3 expansion regions of 28S rRNA, internal transcribed spacer (ITS) rRNA, partial 18S rRNA gene, the protein-coding mitochondrial gene, cytochrome oxidase *c* subunit I (*COI*), and the heat-shock protein 90 (*hsp90*) gene, support the new species status. The results of a host-suitability test indicated that the new species does not parasitize potato (*Solanum tuberosum*) tubers and broad bean (*Vicia faba*) seedlings. Histopathological observations on naturally infected sowthistle tissues revealed that *D. oncogenus* n. sp. causes floral stem neoplasia and midrib leaf gall formation on

*Fax: +34957499252
E-mail: p.castillo@csic.es

the type, and to date only known, host. The galls were characterized by extensive hyperplasia, where several necrotic cells in the neoplasic area were directly damaged by feeding of the nematode, whereas a number of adjacent cells showed typical cytological changes, such as granulated cytoplasm with hypertrophied nuclei and nucleoli.

Introduction

Among more than 60 species presently recognized in the genus *Ditylenchus* Filipjev, 1936 (Siddiqi, 2000; Vovlas *et al.*, 2011), only a few are parasites of higher plants, while the majority of species are mycophagous (Sturhan & Brzeski, 1991). Plant-parasitic *Ditylenchus* species are migratory endoparasites in above-ground parts of plants or into roots, stolons, tubers and rhizomes, causing dissolution of the middle lamellae of the cell walls so that cells become detached and the tissue swells (Sturhan & Brzeski, 1991). *Ditylenchus* spp. tend to be greatly conserved in gross morphology, which makes species identification a very difficult task (Brzeski, 1991). Since species identification of nematodes has traditionally been based on the morphological or typological species concepts, molecular techniques have recently shown that many presumed monospecific species are in fact sibling or cryptic species, genetically distinct but sharing similar morphology (Subbotin *et al.*, 2005). Accordingly, the nematode species concept has been discussed recently, suggesting that delimitation of species should be based mainly on an amalgamation of principles of polyphasic taxonomy, which assembles and assimilates all available data and information (phenotypic, genotypic and phylogenetic) used for delimiting taxa at all levels (Subbotin & Moens, 2006).

The type species of the genus is the stem and bulb nematode, *Ditylenchus dipsaci* (Kuhn, 1857) Filipjev, 1936, which is a severe plant pathogen worldwide. The phylogenetic analysis of rRNA gene sequences of different populations and races of stem and bulb nematode resulted in several species previously identified under the name *D. dipsaci* (Subbotin *et al.*, 2005). Presently, the *D. dipsaci* species complex contains the following species: *D. dipsaci* (*sensu stricto*), *D. weischeri* Chizhov *et al.*, 2010, *D. gigas* Vovlas *et al.*, 2011, and several still undescribed species, namely *Ditylenchus* sp. D from *Pilosella* spp., *Ditylenchus* sp. E from *Crepis praemorsa* (L.) Tausch, *Ditylenchus* sp. F from *Hieracium pilosella* L. and *Scorzoneroides autumnalis* (L.) Moench, and *Ditylenchus* sp. G from *Plantago maritima* L. Recently, *Ditylenchus arachis* Zhang, Liu, Janssen, Zhang, Xiao, Li, Couvreur and Bert, 2014 has been described from peanut fields, inducing peanut pod rot in China (Zhang *et al.*, 2014).

During a nematode survey on natural vegetation from the Adriatic coast in the locality Pantanagianni, of Brindisi province in southern Italy, an unknown species of stem nematode belonging to the genus *Ditylenchus* was detected in leaves and stems of sowthistle, *Sonchus bulbosus* (L.) N. Kilian & Greuter from the family Asteraceae. This plant species is a common weed, widely distributed in coastal vegetation from Italy and other countries of south-eastern Europe. Tuberous sowthistle floral stems and leaf midribs infected by the nematode appeared discoloured and clearly deformed due to the presence of tumours developed by the intensive cell proliferation stimulated during nematode feeding activity. There are several reports on nematode infections of *Sonchus* species*: S. arvensis*, *S. bulbosus*, *S. oleraceus* infected by *D. dipsaci* and *D. sonchophilus* Kirjanova, 1958 (Goodey *et al.*, 1965; Teploukhova, 1968).

The objectives of the present study were to: (1) identify the leaf and stem nematode species infecting sowthistle in southern Italy; (2) characterize molecularly a stem nematode population using the D2–D3 expansion segments of 28S rRNA, internal transcribed spacer sequence (ITS), partial 18S rRNA, cytochrome oxidase *c* subunit 1 (*COI*) and heat-shock protein 90 (*hsp90*) gene sequences; (3) explore the phylogenetic relationships of this stem nematode within other *Ditylenchus* and Anguinidae representatives; (4) provide morpho-biological information on the host–parasite relationships of this nematode species with the type host (currently the only one known); and (5) determine the host suitability of this nematode population in potato and broad bean, under glasshouse conditions.

Materials and methods

Morphological identification

Four samples of infected stem and leaves of bulbous sowthistle were collected from coastal sand dunes in Pantanagianni, Brindisi province in southern Italy. Nematodes were extracted from floral stem or leaf swellings (fig. 1), collected in the winter (January–February) at the type locality. Hypertrophied tissues were selected, sections 0.5–0.8 mm thick were cut and incubated in water in Petri dishes. After incubation for 2–3 h, the nematode specimens that emerged were used for morphological observations and molecular analysis. For diagnostics and identification, extracted nematodes were narcotized by gentle heat, and mounted in water agar (Esser, 1986).

Adult specimens for microscopic observation were killed by gentle heat, fixed in a solution of 4% of formaldehyde +1% propionic acid, and processed to glycerol according to Seinhorst's method (Hooper, 1986). Glycerin-infiltrated specimens were examined by light microscopy for diagnosis. Specimens mounted on water agar temporary slides (Troccoli, 2002) were photographed with a Leica DFC 425 system mounted on a Leitz Wetzlar optical microscope (Milano, Italy), whereas measurements and drawings of glycerin-infiltrated specimens were made with a *camera lucida*. Specimens fixed in formaldehyde (4% solution) were dehydrated in an ethanol gradient, critical-point dried, sputter-coated with gold and observed by scanning electron microscopy (SEM) according to Abolafia *et al.* (2002).

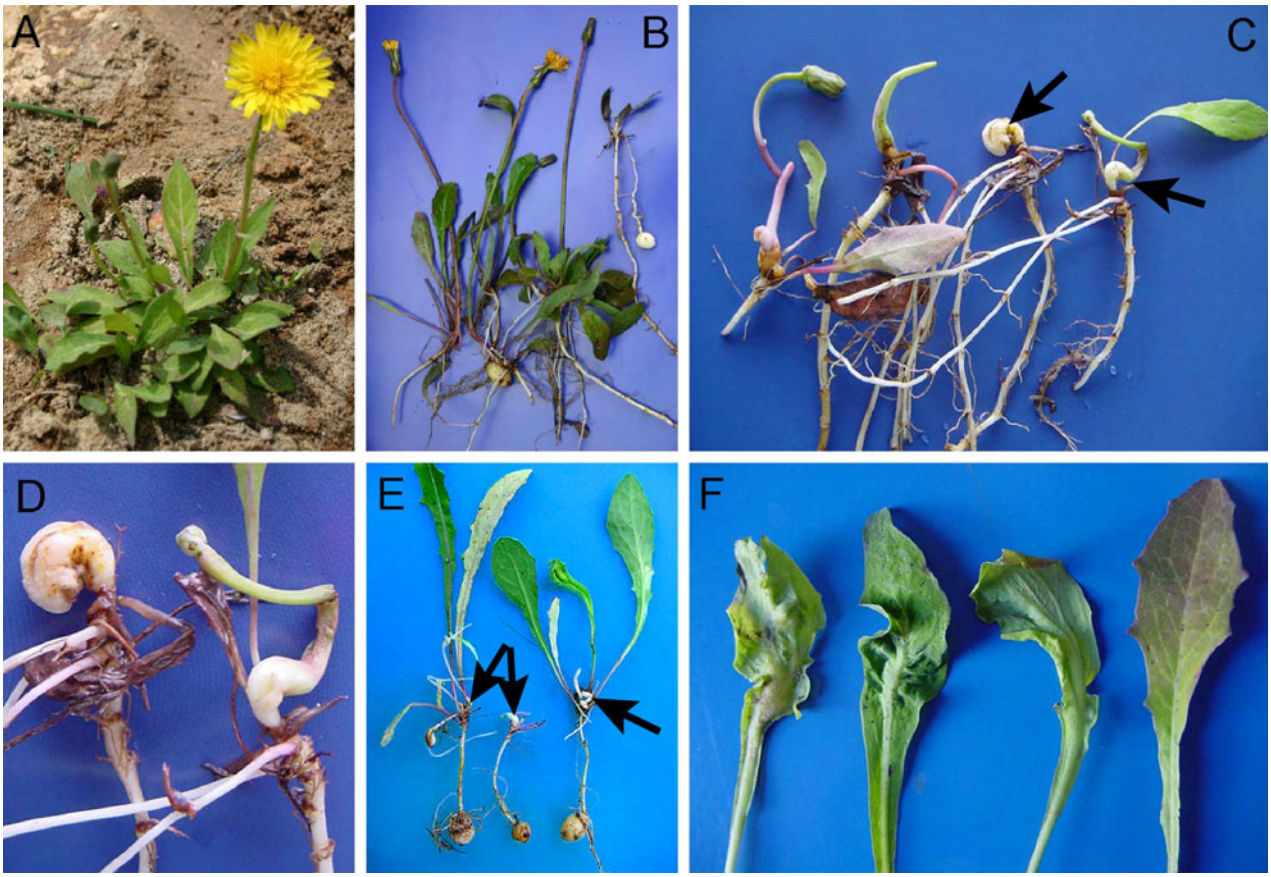

Fig. 1. Symptomatology of damage caused by *Ditylenchus oncogenus* n. sp. on *Sonchus bulbosus*. (A, B) Type host plants, showing healthy flower stems and leaves. (C) Neoplasic tissues (galls arrowed), induced by the nematode endoparasitic feeding activity. (D) Close-up of tumour formations due to the cell proliferation following nematode chemical stimuli. (E) Young nematode-infected plants, showing early gall formation (arrowed). (F) Leaf midrib nematode-induced galls, showing different deformation degrees.

Molecular identification

For molecular analyses, a young female from a bulbous sowthistle infected leaf was mounted temporarily in a drop of 1M NaCl containing glass beads, then mounted on water-agar substrate and, after taking measurements and photomicrographs of diagnostic characters, the slide was dismantled and DNA extracted. Nematode DNA was extracted from this single individual female nematode and polymerase chain reaction (PCR) assays were conducted as described by Castillo *et al.* (2003). The D2–D3 expansion segments of 28S rDNA were amplified using the D2A (5′-ACAAGTACCGTGAGGGAAAGTTG-3′) and D3B (5′-TCGGAAGGAACCAGCTACTA-3′) primers (Castillo *et al.* 2003). The ITS region was amplified using forward primer TW81 (5′-GTTTCCGTAGGTGAACCTGC-3′) and reverse primer AB28 (5′-ATATGCTTAAGTTCAGCGGGT-3′), as described in Subbotin *et al.* (2001); and the partial 18S rRNA was amplified using primers A (5′-AAAGATTAAGCCATGCATG-3′), 13R (5′-GGGCATCACAGACCTGTTA-3′) and 18P-SSU_R_81 (5′-TGATCCWKCYGCAGGTTCAC-3′) (Boutsika *et al.*, 2004). The portion of the *COI* gene was amplified as described by Gulcu *et al.* (2008) using forward primer COIFIC_Fw (5′- CCTACTATGATTGGTGGTTTTGGTAATTG -3′) and reverse primer COIFIC_Rv (5′-GTAGCAGCAGTAAAATAAGCACG -3′). Finally, the portion of the *hsp90* gene was amplified using primers U831 (5′-AAYAARACMAAGCCNTYTGGAC-3′) and L1110 (5′-TCRCARTTVTCCATGATRAAVAC-3′) (Skantar & Carta, 2005).

PCR products were purified after amplification using ExoSAP-IT (Affymetrix, USB products, High Wycombe, Bucks, UK). For the partial *hsp90* gene, the PCR product was cloned into the pGEM-T Easy vector (Promega Corporation, Madison, Wisconsin, USA) and transformed into *Escherichia coli* JM 109 High Efficiency Cells (Promega Corporation) according to the manufacturer's instructions. Several *E. coli* colonies were studied using PCR analysis with the primers used in their respective PCR. The plasmid DNA containing the insert from the positive *E. coli* colonies or PCR products were quantified using a Nanodrop spectrophotometer (Nanodrop Technologies, Wilmington, Detroit, USA) and used for direct sequencing in both directions using the primers referred to above. The resulting products were purified and run on a DNA multicapillary sequencer (Model 3130XL genetic analyser; Applied Biosystems, Foster City, California, USA),

Table 1. Morphometrics of *Ditylenchus oncogenus* n. sp. All measurements in μm and in the form: mean ± SD (range).[a]

	Holotype	Females	Males
n	1	20	15
L	1067	1119 ± 45.0 (1008–1174)	1029 ± 65.3 (862–1127)
Stylet length	9.5	9.5 ± 0.4 (9.0–11.0)	9.5 ± 0.6 (8.0–10.0)
Stylet conus	4.5	4.5 ± 0.3 (4.0–5.0)	4.6 ± 0.3 (4.0–5.0)
DGO	2.0	1.5 ± 0.3 (1.0–2.0)	1.5 ± 0.3 (0.7–2.0)
V or T (%)	81.4	83.4 ± 1.4 (81–86)	72.0 ± 7.4 (55.0–84.3)
Anterior end to:			
centre of metacorpus	53	62.0 ± 7.5 (56–85)	59.0 ± 6.3 (40–67)
end of pharyngeal gland lobe	163	160 ± 10.7 (143–184)	156 ± 14.5 (111–172)
secretory/excretory pore	133	126 ± 11.4 (96–149)	129 ± 13.6 (86–146)
Pharyngeal isthmus	53	50 ± 9.3 (39–79)	50 ± 6.2 (37–61)
Maximum body diameter	32.5	33.0 ± 2.6 (27.0–36.0)	23.5 ± 1.9 (21.0–27.0)
Vulval body diameter	28.0	27.0 ± 1.9 (23.0–31.5)	–
Vulva–anus distance	127	123 ± 14.3 (101–157)	–
PUS	82.0	79.5 ± 10.6 (60.0–97.0)	–
Tail length	72.0	61.0 ± 6.2 (51.5–72.0)	59.0 ± 3.6 (53.0–67.0)
Anal body diameter	16.0	14.0 ± 1.1 (13.0–16.0)	14.0 ± 0.7 (13.5–15.5)
Spicule length	–	–	22.5 ± 1.2 (20.0–24.0)
Gubernaculum length	–	–	7.5 ± 0.9 (6.0–9.0)
a	32.7	34.3 ± 3.6 (28.0–42.3)	43.7 ± 2.9 (38.0–48.1)
b	6.6	7.1 ± 0.5 (6.1–8.0)	6.7 ± 0.9 (5.0–9.2)
c	14.8	18.6 ± 2.0 (14.8–22.3)	17.5 ± 1.7 (14.8–19.7)
c	4.5	4.3 ± 0.4 (3.3–5.2)	4.2 ± 0.3 (3.8–4.8)

[a] All abbreviations used are defined by Siddiqi (2000).

at the STABVIDA sequencing facilities (Caparica, Portugal). The newly obtained sequences were submitted to the GenBank database under accession numbers KF612015–KF612019.

Phylogenetic analysis

The D2–D3 of 28S rRNA, ITS, 18S rRNA, *COI* and *hsp90* gene sequences of different Anguinidae from GenBank were used for phylogenetic reconstruction. The following outgroup taxa for D2–D3 segments of 28S, ITS, 18S, *COI* and *hsp90* datasets were selected: *Bursaphelenchus xylophilus* (DQ364687, JQ743665), *Aphelenchoides fragariae* (AY508034), *Xiphinema pachtaicum* (JQ990057), *Psilenchus minor* (EU915499), and *Cephalenchus hexalineatus* (EU915495), respectively. The newly obtained and published sequences for each gene were aligned using Clustal W (Thompson *et al.*, 1994) with default parameters. Sequence alignments were edited manually using BioEdit (Hall, 1999). Phylogenetic analyses of the sequence datasets were performed with maximum likelihood (ML) using PAUP* 4b10 (Swofford, 2003) and Bayesian inference (BI) using MrBayes 3.1.2 (Huelsenbeck & Ronquist, 2001). The best fitted model of DNA evolution was obtained using jModelTest v. 2 (Darriba *et al.*, 2012) with the Akaike information criterion (AIC) and included in the phylogenetic analyses. BI analysis for D2–D3 expansion segments of 28S rDNA, ITS and partial 18S regions under the GTR +G, TVM +G, GTR +I + G, GTR +G and TPM2 + G models, respectively, were initiated with a random starting tree and run with the four Metropolis-coupled Markov chain Monte Carlo (MCMC) methods for 1×10^6 generations, with the exception of the ITS region with 2×10^6 generations. The MCMC were sampled at intervals of 100 generations. Two runs were performed for each analysis. After discarding burn-in samples and evaluating convergence, the remaining samples were retained for further analyses. The topologies were used to generate a 50% majority rule consensus tree. Posterior probabilities (PP) and bootstrap support (BS) are given on appropriate clades. Trees were visualized using TreeView (Page, 1996). In ML analysis the estimation of the support for each node was obtained by bootstrap analysis with 100 replicates and fast-step replicates.

Histopathology

For histopathological observations, naturally infected (hypertrophied) stem tissues and leaf galls of bulbous sowthistle were gently washed free of adhering soil and debris. Infected hypertrophied tissues, galls and healthy stem pieces were cut into segments 3 mm wide ×5 mm long, fixed in FAA (formaldehyde–acetic acid–alcohol) for a minimum of 48 h, dehydrated in tertiary butyl alcohol series (40–70–85–90–100%) and embedded in Histosec® embedding paraffin, melting point 56–58°C (Merck, Darmstadt, Germany). Embedded tissues were sectioned transversely and longitudinally at 10–12 μm with a rotary microtome, mounted on glass slides, stained with safranin and fast green (Johansen, 1940), mounted permanently in a 40% xylene solution of a polymethacrylic ester (Synocril 9122X, Cray Valley Products, New Jersey, USA) and observed with an optical microscope. Images were taken with a Leica DFC 425 system.

Host-suitability test

Due to morphological similarities of this species with the two main phytopathogenic species of this genus, namely *Ditylenchus destructor* and *D. dipsaci* (Thorne, 1945), species of quarantine importance whose main hosts are potato and broad bean, respectively, a host-suitability test of *D. oncogenus* n. sp. was performed in order to test the suitability of these two host plants for the new stem and leaf nematode species.

For that purpose, potato (*Solanum tuberosum* L.) cv. Spunta tubers and broad bean (*Vicia faba* L.) cv. Acquadulce seeds were surface disinfested with 2% NaOCl for 3 min and germinated on sterile, moistened filter paper in Petri dishes. These potato and broad bean cultivars were selected as susceptible hosts of *D. destructor* and *D. dipsaci* (or *D. gigas*), respectively (Brzeski, 1991). Disinfested seeds were sown in 250-cm^3 clay pots (four replicates per each host, 12 overall repetitions) containing artificially infested soil with this stem and leaf nematode at a density of 12 specimens/ml of soil. Plants in pots were watered as needed and fertilized once a week with 100 ml of a hydro-sol fertilizer solution (0.1%, 20–5–32 + micronutrients) (Haifa Chemicals Ltd, Haifa, Israel). The pots were maintained in glasshouse conditions at 20 ± 5°C for 4 months. After that, broad bean seedlings and the newly formed potato tubers were removed from the pots, and nematode populations were evaluated after extraction, using a magnesium sulphate ($MgSO_4$) maceration–centrifugal flotation method (Coolen, 1979).

Results and discussion

Description of Ditylenchus oncogenus *n. sp.*
(Order: Tylenchida; Family: Anguinidae)

Morphology

Female (figs 2–5, table 1). Body almost straight when heat relaxed. Lip region relatively high, measuring 2.6 ± 0.3 (2.0–3.0) and 6.5 ± 0.3 (6.0–6.5) µm in height and width, respectively. By light microscopy, lip region contour appearing almost smooth, with only a basal annulus discernible and an oral disc slightly raised in most of the specimens. In '*en face*' view on SEM, labial

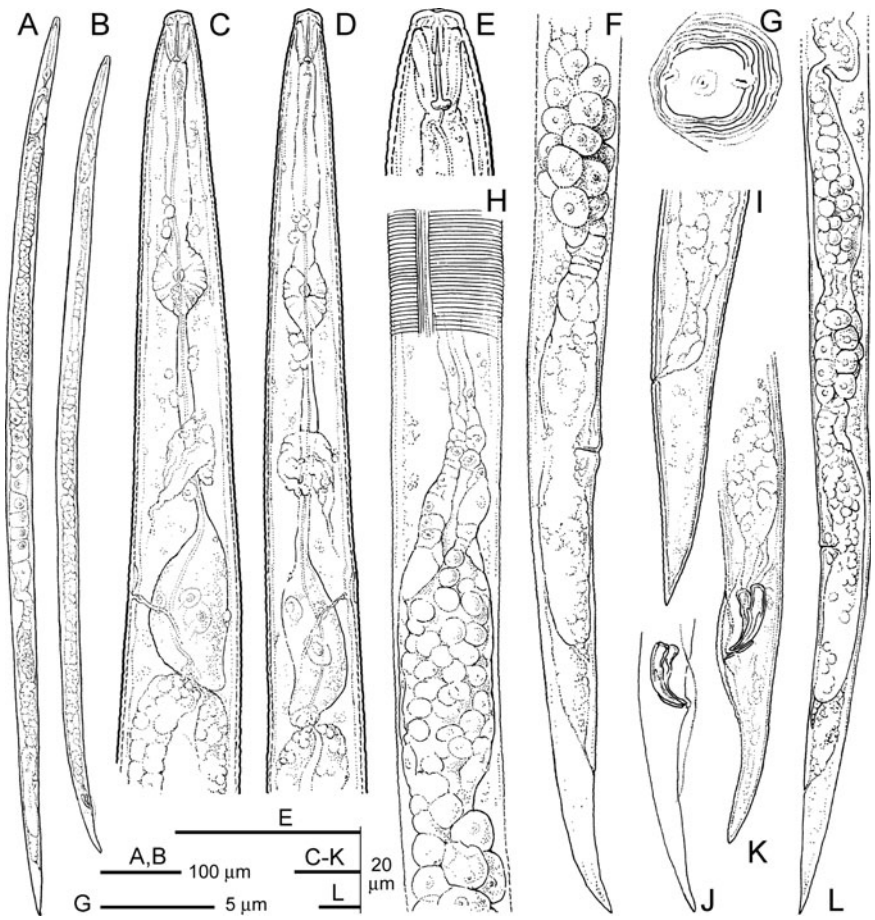

Fig. 2. *Ditylenchus oncogenus* n. sp., illustrating main morphological details of taxonomic value: (A, B) female and male entire body; (C, D) female and male pharyngeal region; (E) female lip region; (F) female quadricolumella and post-vulval region; (G) outline of female lip region in *en face* view (as seen at SEM); (H) female spermatheca with lateral field view; (I) female tail; (J, K) male tail; (L) female posterior body region.

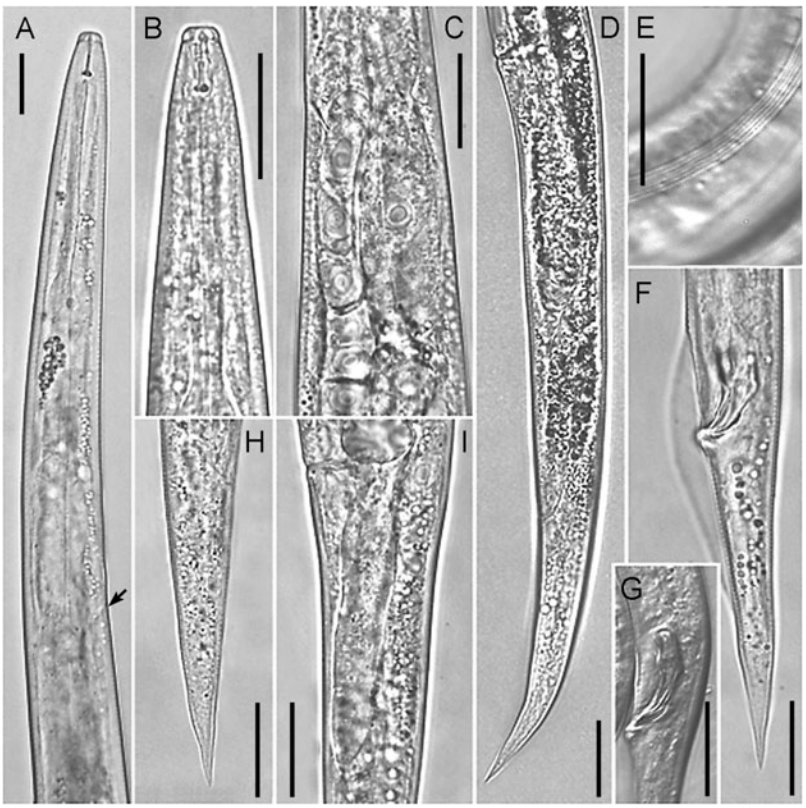

Fig. 3. *Ditylenchus oncogenus* n. sp.: (A) pharyngeal region, with arrowed the excretory pore position; (B) female anterior end; (C) female glandular pharyngeal bulb with partly overlapped germinal zone of the ovary; (D) female body portion posterior to vulva; (E) lateral field at midbody, showing six incisures; (F) male tail; (G) male spicules; (H) female tail; (I) female post-uterine sac. Scale bars = 20 μm.

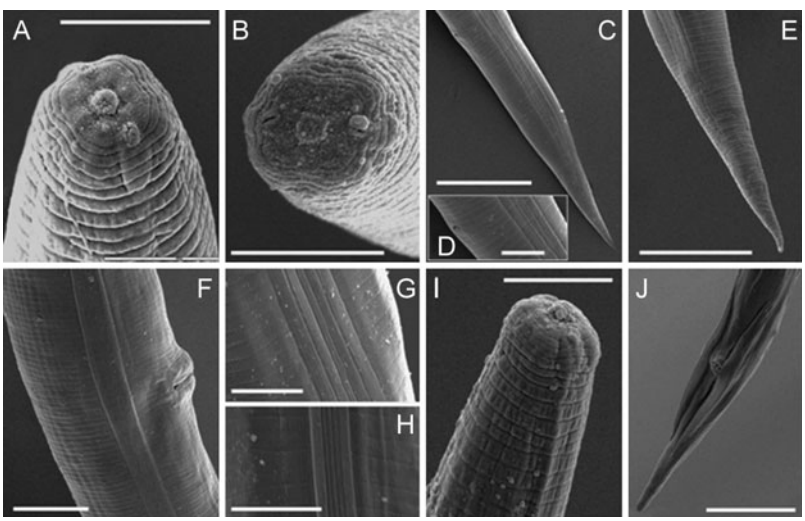

Fig. 4. Scanning electron micrographs of *Ditylenchus oncogenus* n. sp.: (A, B) female lip region, with view (in B) of amphidial apertures; (C) female tail region; (D) enlarged detail of (C), showing crescentic anal aperture; (E) female tail tip; (F) female vulval region; (G, H) detail of female (G) and male (H) lateral field at midbody, showing six plain incisures; (I) male anterior end; (J) male tail in ventro-sublateral view, showing a leptoderan bursa flanking the cloacal aperture. Scale bars: A, B, D, G, H, I = 5 μm; E, F = 10 μm; C, J = 20 μm.

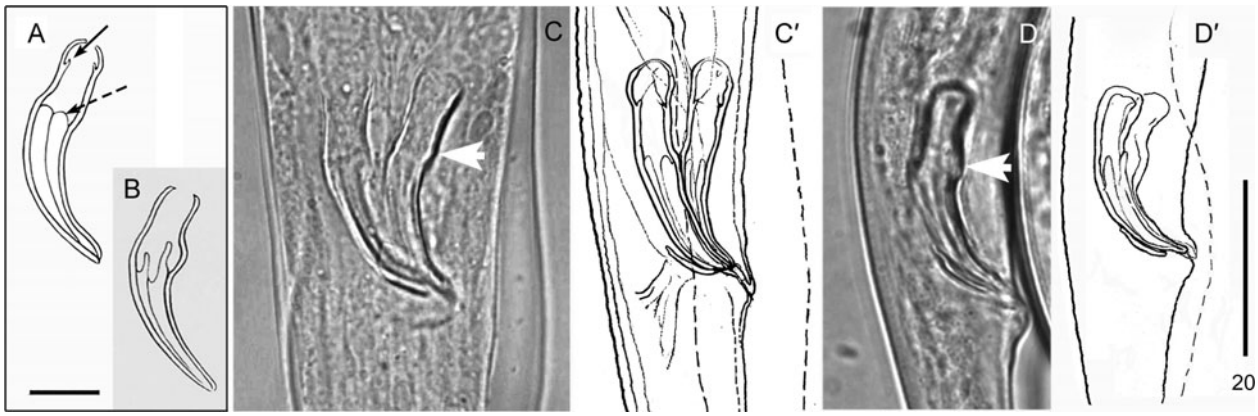

Fig. 5. Comparative spicule pattern design in four *Ditylenchus* spp.: (A, B) *D. dipsaci* and *D. destructor* (from Karssen & Willemsen, 2010, modified); (C, C′) *D. gigas*; (D, D′) *D. oncogenus* n. sp. The black solid arrow indicates the minute processes at the base of the manubrium; the black dashed arrow indicates the velum within the lamina; white arrows show the more or less prominent tumulus in the calomus area. Scale bars: A = 8 μm; D′ = 20 μm.

area smooth, of quadrangular outline, composed of three annuli. Stoma opening pore-like at the centre of a small oral disc. Amphidial openings slit-like, nearly horizontal or dorso-laterally oriented, protruding laterally. Cuticle annuli 1.1–1.5 μm wide at midbody. Stylet delicate, with minute, roundish knobs, often flattened anteriorly, 2.5 ± 0.4 (1.5–3.0) μm across. Dorsal gland orifice (DGO) 13.6 ± 3.7 (6.9–21.4)% of stylet length. Pharyngeal procorpus cylindrical, with a slight constriction at the junction with median bulb. Metacorpus mostly oval in shape, 16.5 ± 1.2 (13–18) μm and 10.5 ± 0.7 (9.5–12.0) μm in longitudinal and cross diameter, respectively. Isthmus long, slender, crossed nearly in the middle by the nerve ring. Basal pharyngeal bulb saccate. A slight overlap over intestine, ranging from 1.5 to 9.0 μm, was detected in a few specimens only. Hemizonid located at mid-level of pharyngeal basal bulb, about three cuticular annuli long. Secretory–excretory pore immediately, or one annule, posterior to hemizonid. Lateral fields with six plain incisures (figs 2H and 3E), often difficult to see under the light microscope. Ovary mono-prodelphic, well developed. Anterior genital tract 745 ± 90.9 (530–882) μm long, 67 ± 7.4 (53–77)% of body length, with the apex of germinal zone sometimes reaching the middle of pharyngeal basal bulb. Spermatheca broad, elongated, mean 86 ± 24.5 (38–123) μm long, 24.0 μm wide, filled with round sperm. Anterior part of uterus in form of a quadricolumella, followed by a short, narrower tract and ending in a swelled posterior part near vagina. Post-vulval uterine sac well developed, 3.0 ± 0.4 (2.2–3.9) times the vulval body diameter; 65 ± 10.4 (41–82)% the vulva–anus distance; rudimentary genital cells are usually present in the posterior end. Tail conoid, ending in a finely pointed terminus. Phasmids distant in mean 33 and 28 μm from tail terminus and from anus, respectively.

Male (figs 2–5, Table 1). Slightly smaller than female, but similar in shape, except in reproductive system. Lip region 2.4 ± 0.3 (2.0–3.0) μm high, 6.2 ± 0.3 (6.0–7.0) μm wide, slightly narrower than the rest of the body. Labial region relatively higher than in female, composed of five annuli; oral disc, separated by fused medial and lateral sectors by a slight incisure, as observed at SEM (fig. 4I). Stylet delicate, knobs small, roundish, 2.0–2.5 μm across. DGO 14.4 ± 3.3 (7–21)% of stylet length. Median bulb oval, of mean length 15.5 and 9.5 μm in longitudinal and cross diameter, respectively. Isthmus slender, elongate, 50 ± 6.2 (37–61) μm long, crossed by nerve ring about in the middle. Basal pharyngeal bulb almost cylindrical, not overlapping intestine. Lateral fields with six smooth incisures (fig. 4H). Testis well developed, 743 ± 97.1 (544–888) μm long, in several specimens extending anteriorly to the base of the pharyngeal bulb. Bursa leptoderan, slightly longer than tail in overall extension, starting anterior to the cloaca at a distance nearly twice the anal body diameter and including 62–67% of tail length. Spicules ventrally arcuate, slightly cephalated anteriorly. Gubernaculum simple, sometimes slightly wavy in its proximal part (fig. 5D).

In a recent study, Karssen & Willemsen (2010) confirmed Thorne's (1945) observations about the clear morphological differences in spicule shape between *D. dipsaci* and *D. destructor*, the latter differing from *D. dipsaci* in having a ventral tumulus in the calomus area and anteriorly pointed, less sclerotized, cuticle parts present within the lamina (fig. 5). Male spicules of *D. oncogenus* n. sp. are similar to those of *D. destructor*.

Type host and location

Holotype female and paratypes were obtained from infected stem tissues of *Sonchus bulbosus* (L.) N. Kilian & Greuter collected by the first author at Pantanagianni, Brindisi province, southern Italy (latitude 40°45′60″N; longitude 17°43′62″E, at sea level), on sandy soil. This species is molecularly conspecific with *Ditylenchus* sp. F (*sensu* Subbotin *et al.*, 2004) which was found parasitizing *Hieracium pilosella* L. in Hirmuste, Estonia, and *Scorzoneroides autumnalis* (L.) Moench in Parniku, Estonia.

Type materials

Holotype, female and male paratypes, mounted on glass slides were deposited in the nematode collection at the Istituto per la Protezione Sostenibile delle Piante (IPSP), CNR, Bari, Italy, and Instituto de Agricultura

Sostenible, CSIC, Córdoba, Spain. Additional paratypes were distributed to the United States Department of Agriculture Nematode Collection, Beltsville, Maryland, USA; the University of California Riverside Nematode Collection, Davis, California, USA; and WaNeCo, Plant Protection Service, Wageningen, The Netherlands.

Etymology

The specific epithet is derived from the ancient Greek '*onkos*', which means bulk, mass, neoplasia, tumour, swelling, gall; and '*genus*' = genesis, meaning formation, inducing; and refers to the characteristic ability of this species to induce this host reaction in the aerial parts of the plant.

Diagnosis and relationships with other species

Ditylenchus oncogenus n. sp. can be distinguished from all other *Ditylenchus* spp. by several morphological and molecular characteristics, as well for its distinct ability to induce active cell proliferation at feeding sites, and distinct epigeal galls, which twist the infected parts of symptomatic plants strongly. The main distinguishing diagnostic characters include the medium body size (1.0–1.2 mm); the lateral fields composed of six incisures with non-areolated bands; the long post-uterine sac; the conical, pointed tail; and the *D. destructor*-like pattern of male spicules.

Ditylenchus oncogenus n. sp. is morphologically and morphometrically similar to *D. sonchophilus* Kirjanova, 1958, which also parasitizes a representative of the genus *Sonchus*, *S. oleraceus*. However, the new species differs from *D. sonchophilus* mainly by the number of lines in lateral fields (six, vs. four in *D. sonchophilus*), shorter stylet (9.0–11.0 vs. 10.9–12.2 μm), slightly shorter female and male body length (1.01–1.17 mm and 0.86–1.13 mm vs. 1.10–1.26 mm and 1.04–1.26 mm, respectively) and slightly shorter male spicules (20–24 vs. 23.3–26 μm). *Ditylenchus sonchophilus* was recorded in two provinces of Georgia and, at present, no molecular characterization of this species has been provided.

Because of its main morphological features, *D. oncogenus* n. sp. should also be compared with *D. dipsaci*, *D. weischeri*, *D. gigas*, *D. dauniae* and *D. destructor*. From *D. dipsaci* it differs mainly in having a slightly shorter body (1.1–1.3 mm in *D. dipsaci*), six vs. four incisures in the lateral fields, and a shorter stylet (10–12 μm in *D. dipsaci*); furthermore, the new species is not able to infect *V. faba*, which is one of primary hosts for *D. dipsaci*. From *D. weischeri* the new species differs in having shorter body (1.37–1.62 mm in *D. weischeri*), six vs. four incisures in the lateral fields, shorter vulva–anus distance (101–157 vs. 172–240 μm), shorter post-vulval uterine sac (60–97 vs. 101–150 μm) and shorter male spicules (20–24 vs. 24–28 μm). From *D. gigas* it differs primarily in body length (1.6–2.0 mm in *D. gigas*), number of incisures in the lateral fields (four in *D. gigas*) and host preference (*V. faba* is the primary host for *D. gigas*). *Ditylenchus dauniae* has a shorter body, stylet and tail length (640–942, 7–8 and 41–62 μm, respectively). This species was described from the rhizosphere of wheat but no endoparasitism was reported, whereas *D. oncogenus* n. sp. induces severe tissue damage on the host plant. Finally, the new species differs from *D. destructor* in having a shorter stylet, posterior pharyngeal bulb with no overlap vs. shortly overlapping, smaller b value (6.1–8.0 vs. 8–10 μm) and different host preferences (potato is not a host for *D. oncogenus* whereas it is a primary host for *D. destructor*).

In addition, *D. oncogenus* n. sp. differs from related species by the specific D2–D3, ITS, 18S rRNA, *hsp90* and *COI* sequences (see below).

Histopathology and host-suitability test

Low population densities of soil infestation (5–40 nematodes per 100 cm^3 of soil, mainly fourth-stage

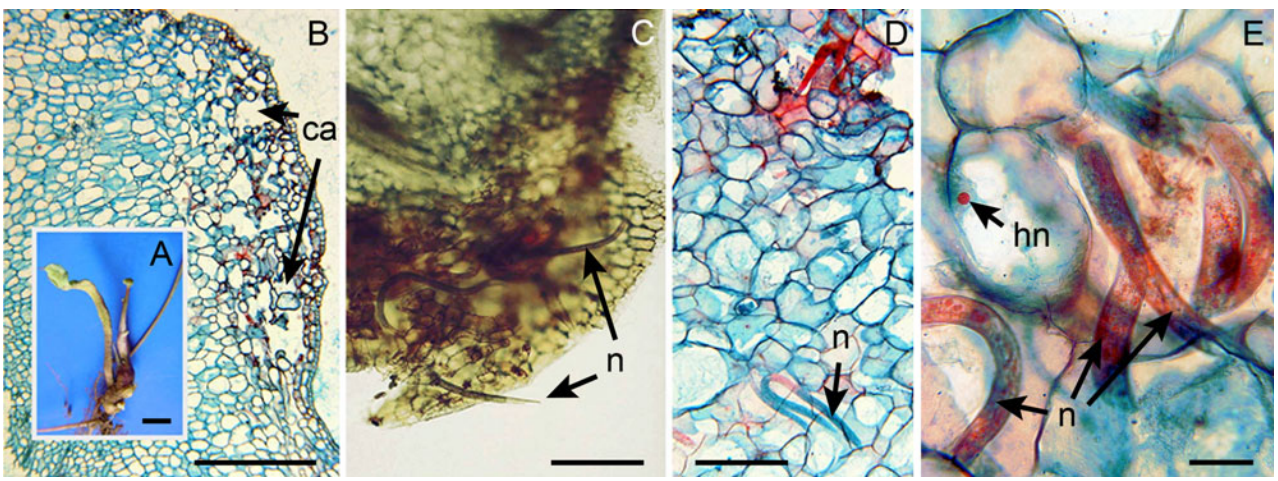

Fig. 6. Histopathological changes induced by *Ditylenchus oncogenus* n. sp. on *Sonchus bulbosus*. (A) Plant and (B) longitudinal section of parenchyma of a stem portion showing sub-epidermal cavities (ca) surrounded by necrotic cells. (C) Cross-section of galled stem with numerous nematode specimens (n). (D, E) Cross-section of flower parenchyma showing a massive nematode presence (n), and hypertrophied nuclei (hn) and nucleoli in the attacked cells. Scale bars: A = 1 mm; B, C = 0.5 mm; D, E = 50 μm.

juveniles (J4), were detected in coastal sand dunes at the type locality. In severely infected plants, differences in size and form of the swellings and galls were observed, detected particularly on floral stems and midrib leaves (fig. 1F). Nematode population densities in infected plant tissues ranged from 15 to 21,945 specimens/g of stem and leaf deformed tissues. Histopathological observations on symptomatic tissues revealed that *D. oncogenus* n. sp. causes floral stem and midrib leaf galls on sowthistle (figs 1 and 6). The galls were characterized by extensive hyperplasia where several necrotic cells in the neoplasic area were damaged directly by the nematode feeding (fig. 6E). However, a number of adjacent cells, not directly penetrated by the nematode stylet, showed some characteristic cytological features, such as granulated cytoplasm with hypertrophied nuclei and nucleoli (fig. 6D, E).

The results of the host-suitability test did not reveal any infection by *D. oncogenus* n. sp. (juvenile or adult specimens) parasitizing the stems of broad beans or potato tubers.

Molecular characterization of Ditylenchus oncogenus *n. sp.*

The amplification of D2–D3 expansion segments of 28S, ITS, partial 18S rRNA, partial *COI* and *hsp90* genes yielded a single fragment of approximately 700, 750, 1600, 400 or 350 bp, respectively, based on estimation using gel electrophoresis. The D2–D3 expansion segments of 28S rRNA gene sequence of *D. oncogenus* n. sp. (KF612015) matched well (98.6–98.5% similarity) with the D2–D3 sequences of *D. gigas* from broad bean and *Ditylenchus* sp. from pea, deposited in GenBank under accession numbers HQ219215 and FJ707364, respectively), differing by 10–11 nucleotides (identities: 729/739, 729/740). The other similar *Ditylenchus* species were *D. dipsaci* from garlic, narcissus and onion (JF327759, FJ707361, HQ219226, respectively) with 96.5–95.7% similarity.

The ITS sequence from *D. oncogenus* n. sp. (KF612016) matched well (99% similarity, one nucleotide difference) with the ITS sequence of *Ditylenchus* sp. F SAS-2004 from *Hieracium pilosella* under the GenBank accession number

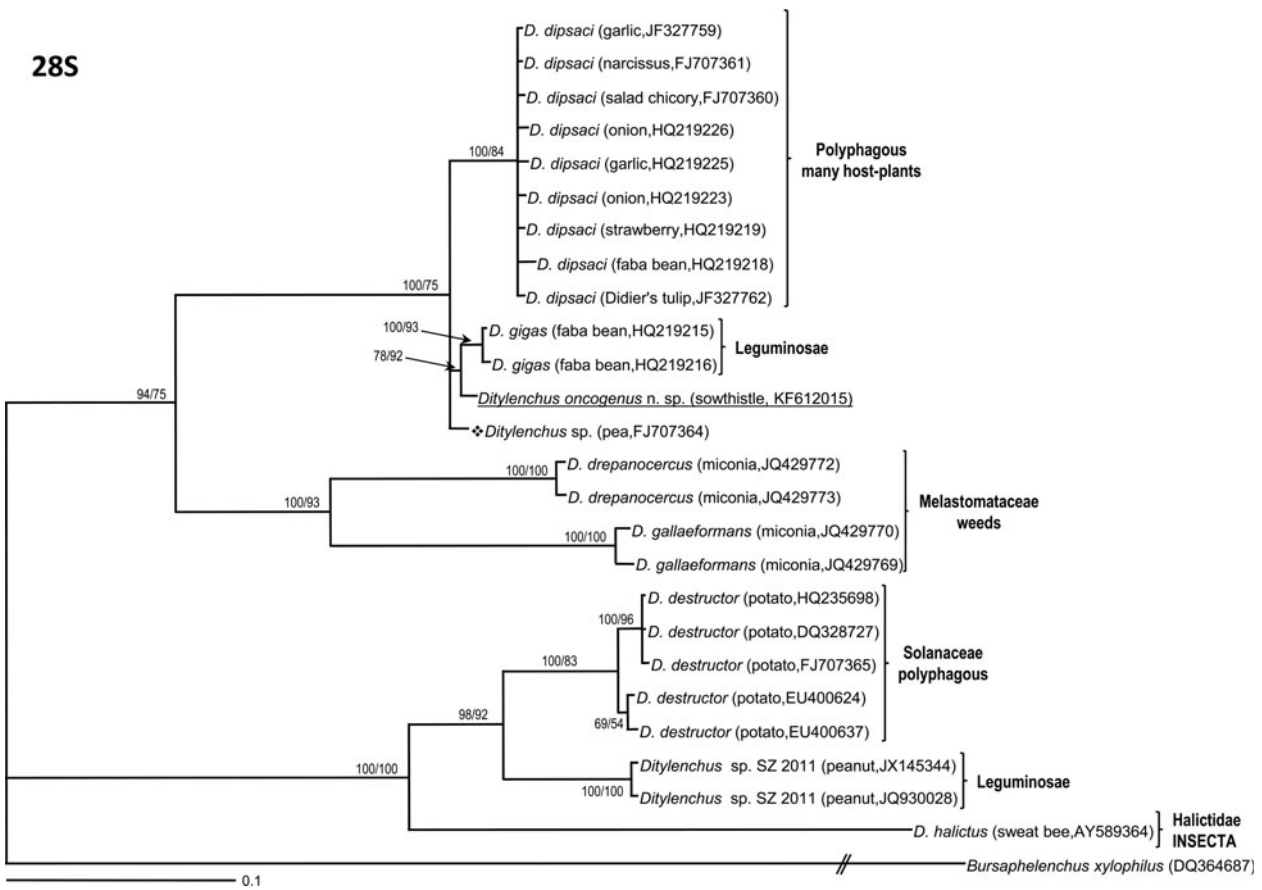

Fig. 7. Phylogenetic relationships within the genus *Ditylenchus*. Bayesian 50% majority rule consensus trees as inferred from D2–D3 expansion segments of 28S rRNA gene sequence alignment under the GTR+G model. Posterior probabilities more than 65% are given for appropriate clades; bootstrap values greater than 50% are given on appropriate clades in ML analysis. Newly obtained sequences in this study are underlined.

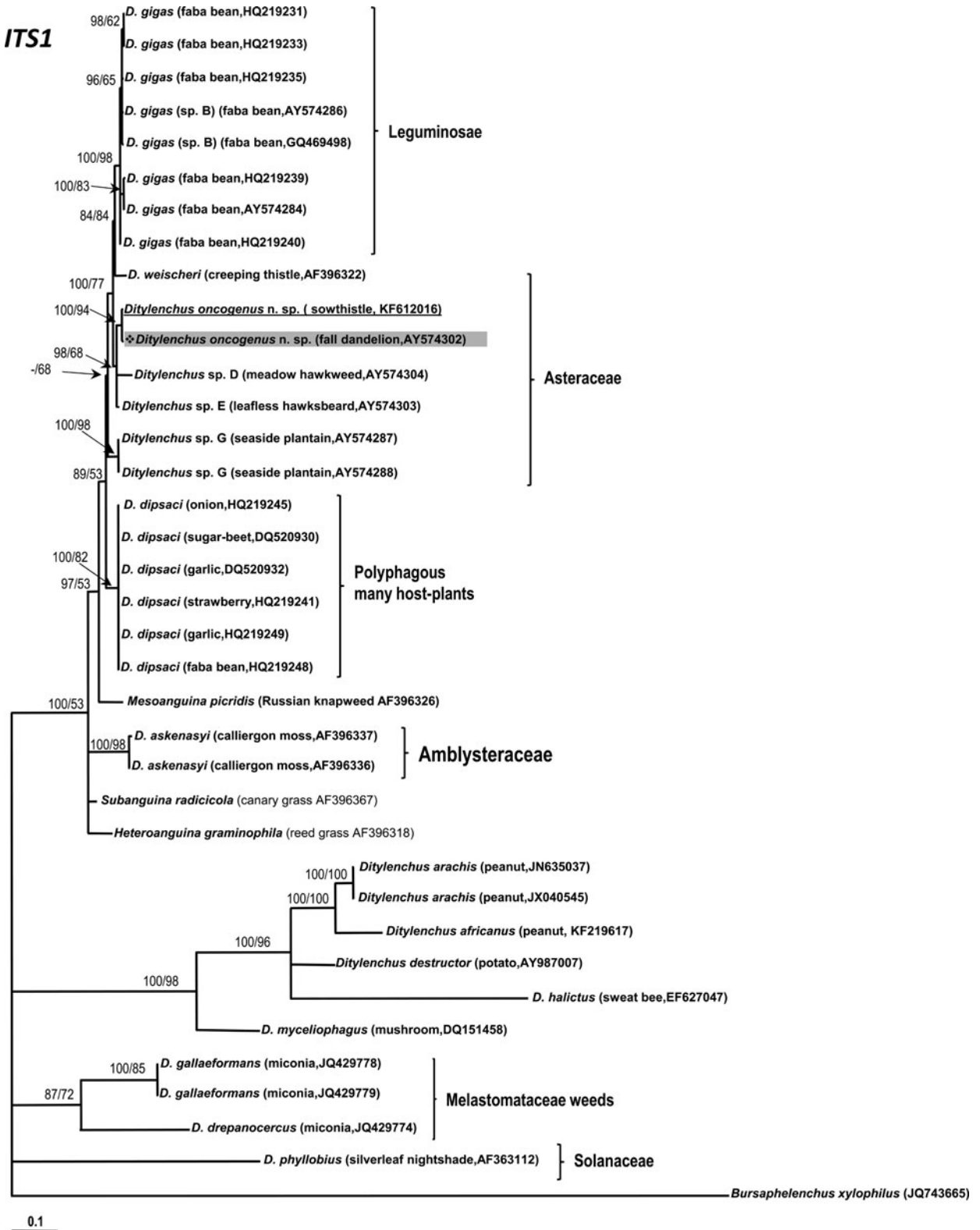

Fig. 8. Phylogeny of the genus *Ditylenchus* and other Anguinidae as inferred from ITS rRNA gene sequence alignment under the TVM+G model. For a description of the tree, see fig. 7.

AY574302. Based on the high sequence similarity, we consider *Ditylenchus* sp. F as conspecific with *D. oncogenus* n. sp. The ITS sequence from *D. oncogenus* n. sp. (KF612016) also matched well with those of several isolates of *D. gigas* (HQ219232–HQ219240), differing by 22–24 nucleotides (identities 900/922 to 898/922) and *D. gigas* (GQ469498) differing by 25 nucleotides (identity 900/925).

The partial 18S rRNA gene sequence (KF612017) was 99% similar to those for several isolates of *D. dipsaci* (see fig. 9) and *D. gigas* (HQ219211), differing by 6–11 nucleotides (identities: 811/817, 806/817) followed by *Subanguina radicicola* (AF202164, EU682392), *Anguina tritici* (AY593913) and *D. drepanocercus* (JQ429768) differing by 19–35 nucleotides (identities: 799/818, 795/817, 786/821, respectively).

The partial *COI* gene sequence (KF612018) was 82% similar to those of *D. gigas* (HQ219213, HQ219214) differing by 111–114 nucleotides (identities: 494/605, 491/605), followed by *D. dipsaci* (HQ219212) and differing by 131 nucleotides (identity: 472/603).

Finally, the partial *hsp90* (KF612019) was 82% similar to those of *D. gigas* (HQ219227– HQ219229), differing by 20 nucleotides (identity: 211/231), followed by *Ditylenchus* sp. G (HM778135, HM778136) and differing by 34 nucleotides (identity: 195/229).

Thus, several gene sequences clearly differentiated *D. oncogenus* n. sp. from closely related *Ditylenchus* spp.

Phylogenetic relationships of Ditylenchus oncogenus *n. sp. with other* Ditylenchus *species*

Phylogenetic relationships among *Ditylenchus* spp. were inferred from analyses of the D2–D3 expansion segments of 28S rRNA, ITS, partial 18S, partial *COI* and partial *hsp90* gene sequences. Trees obtained using BI and ML analyses are given in figs 7–11. No significant differences in topologies were obtained using the BI or ML approaches, except for positions of some species in clades with low BS or PP supports.

The multiple D2–D3 alignment included 26 sequences and was 739 bp in length. The 50% majority rule consensus BI and ML trees consisted of three moderate to highly supported major clades for the genus *Ditylenchus* (fig. 7): (1) four *Ditylenchus* species including *D. dipsaci* from several host plants: *D. gigas* from broad bean, *D. oncogenus* n. sp. (KF612015) from bulbous hawksbeard, and *Ditylenchus* sp. (FJ07364) (PP = 100%; BS = 75%); (2) two *Ditylenchus* species – *D. drepanocercus* (JQ429772, JQ429773) and *D. gallaeformans* (JQ429769, JQ429770) – causing gall-like structures on infected

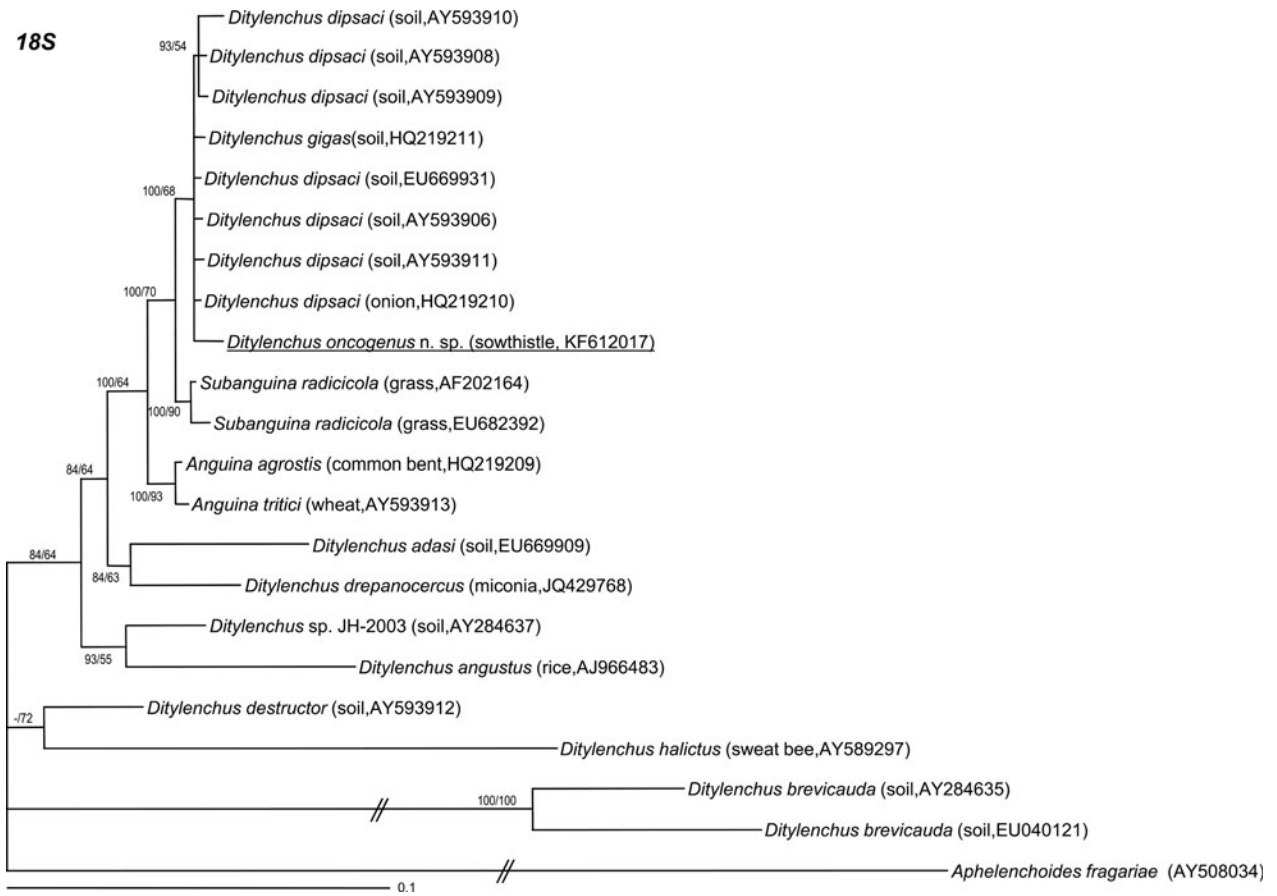

Fig. 9. Phylogenetic relationships within the genus *Ditylenchus* as inferred from partial 18S rRNA gene sequence alignment under the GTR+I+G model. For a description of the tree, see fig. 7.

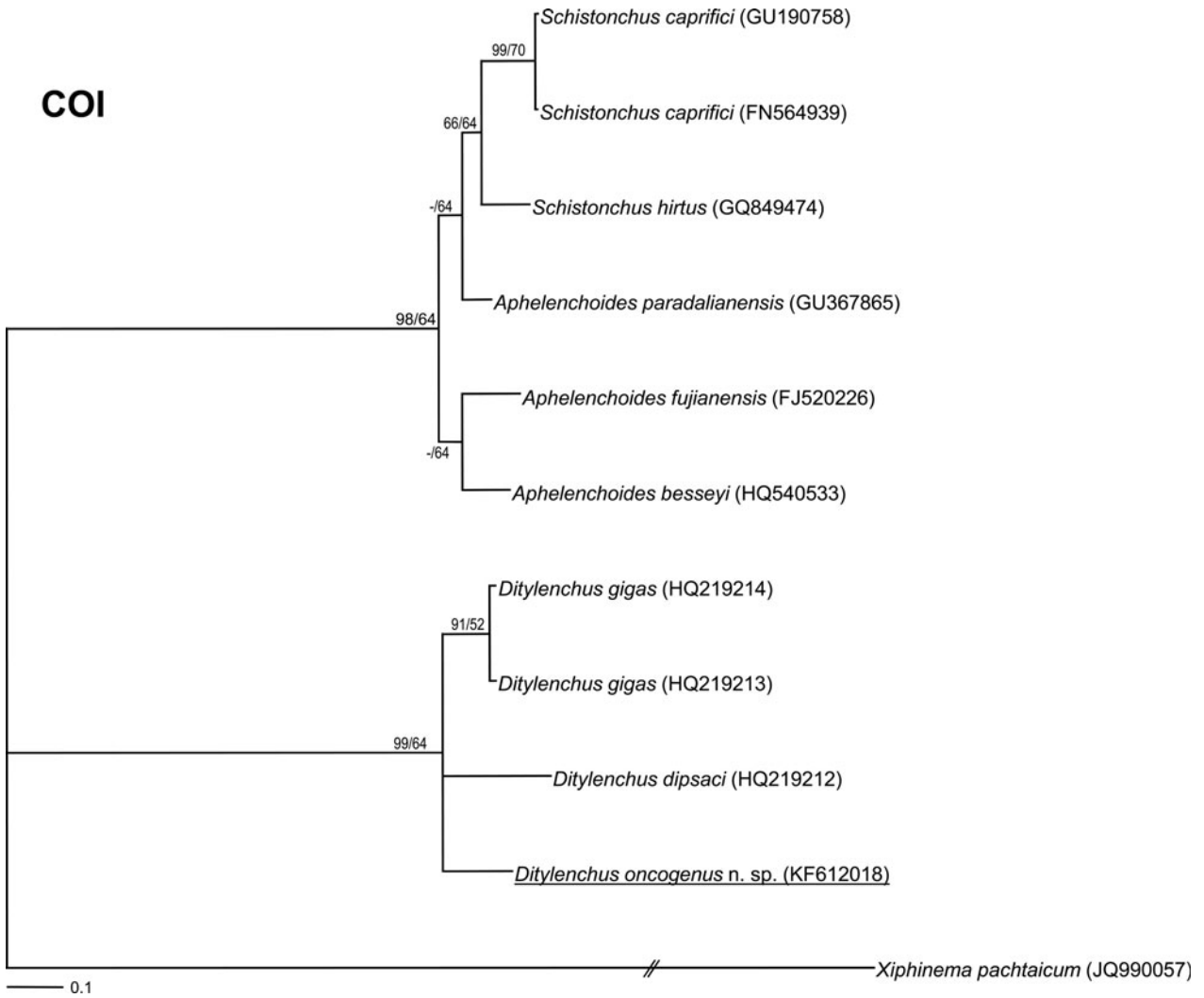

Fig. 10. Phylogenetic relationships within the genus *Ditylenchus* and *Aphelenchoides* and *Schistonchus* spp. generated from the partial *COI* gene dataset with the GTR+G+F model. For a description of the tree, see fig. 7.

leaves of several weed species (PP = 100%; BS = 93%); and (3) three *Ditylenchus* species including *D. destructor* parasitizing potato, *D. arachis* (JX145344, JQ930028) from peanut, and *D. halictus* (AY589364), a phoretic species from sweet bee *Halictus sexcinctus* (Fabricius, 1775) Blüthgen, 1923 (PP = 100%; BS = 100%).

The ITS multiple edited alignment included 36 sequences and was 673 bp in length. Phylogenetic analysis (BI and ML) of *Ditylenchus* spp. (fig. 8) revealed that Italian isolates and Estonian (=*Ditylenchus* sp. F from *Hieracium pilosella,* AY574302) isolates of *D. oncogenus* n. sp. clustered together. These *Ditylenchus* species formed a highly supported clade (PP = 99%; BS = 74%) with other *Ditylenchus* species parasitizing stems and leafs of Asteraceae, including *Ditylenchus* sp. D (AY574304), *Ditylenchus* sp. E (AY574303) and *Ditylenchus* sp. G (AY574287, AY574288). All *D. gigas* isolates parasitizing broad bean formed a highly supported clade (PP = 100%; BS = 98%), with *D. weischeri* (AF396322) parasitizing *Cirsium arvense* (L.) Scop. *Ditylenchus dipsaci* isolates parasitizing several host plants (onion, sugar-beet, garlic, strawberry, and broad bean) also formed a highly supported clade (PP = 100%; BS = 91%). *Ditylenchus gallaeformans* (JQ429778, JQ429779) and *D. drepanocercus* (JQ429774) formed a well-supported clade (PP = 100%; BS = 85%), clearly separated from the previous species. Other *Ditylenchus* spp. (i.e. *D. phyllobius*, *Ditylenchus arachis*, *D. myceliophagus* and *D. destructor*), formed a basal, low-supported clade (PP = 73%; BS = 58%).

The alignment of the 18S rRNA gene was 1694 bp in length and contained 22 taxa, including the outgroup taxa. Phylogenetic analysis of the 18S sequences revealed close relationships of *D. oncogenus* n. sp. with several isolates of *D. dipsaci* and *D. gigas* (PP = 100%; BS = 70%) (fig. 9). Other *Ditylenchus* spp. (including *D. adasi*, *D. drepanocercus*, *Ditylenchus* sp. JH-2003, *D. angustus*, *D. destructor*, *D. halictus* and *D. brevicauda*) were clearly

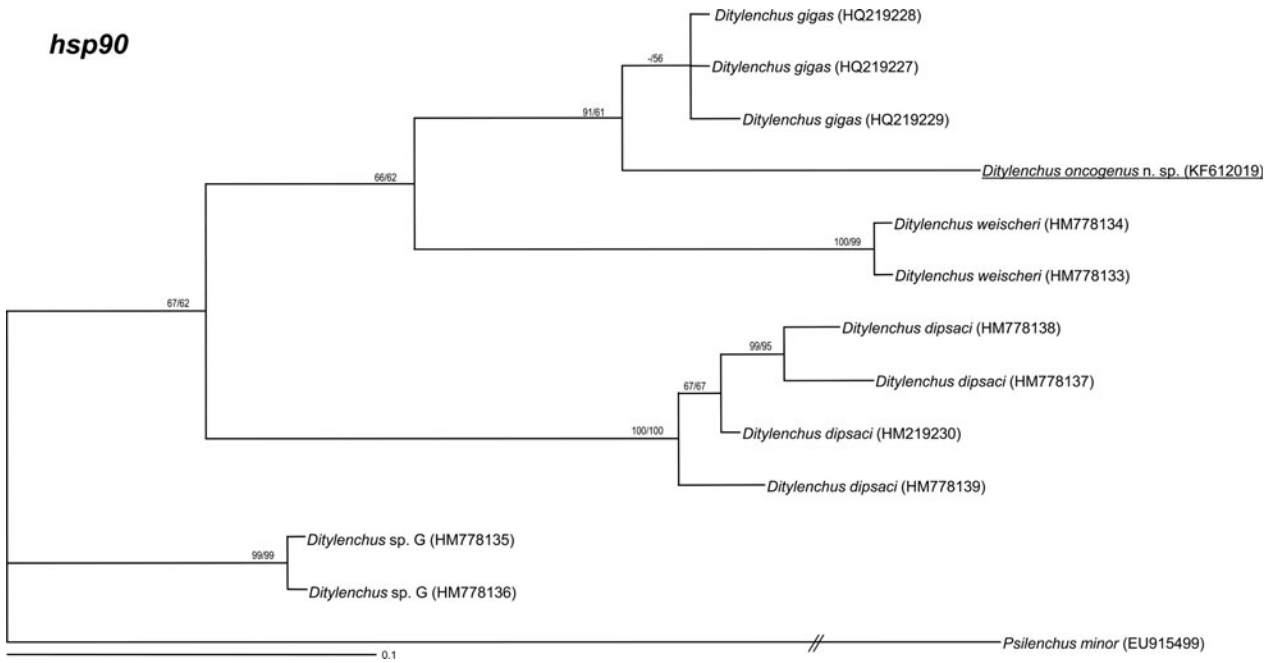

Fig. 11. Phylogenetic relationships within the genus *Ditylenchus* generated from the *hsp90* gene dataset with the TPM2+G model. For a description of the tree, see fig. 7.

separated in four different moderate- to low-supported clades (fig. 9).

The alignment of the partial *COI* gene was 615 bp in length and contained 11 taxa, including the outgroup. Phylogenetic analysis of *COI* sequences revealed close relationships of *D. oncogenus* n. sp. with *D. dipsaci* (HQ219212) and *D. gigas* (HQ219213, HQ219214) (PP = 99%; BS = 64%), clearly separated from the clade formed by *Schistonchus* spp. and *Aphelenchoides* spp. (fig. 10).

Finally, the alignment of the partial *hsp90* gene was 229 bp in length and contained 14 taxa, including the two outgroup taxa. Phylogenetic analysis of *hsp90* sequences revealed close relationships of *D. oncogenus* n. sp. with several isolates of *D. gigas* (PP = 76%; BS = 74%). Other *Ditylenchus* spp. were clearly separated in two clades including several isolates of *D. dipsaci*, *D. weischeri* and a basal clade formed by *Ditylenchus* sp. G (fig. 11).

Our results of the different gene analyses converge and clearly separate *D. oncogenus* n. sp. from *D. gigas*, *D. dipsaci* and other known *Ditylenchus* species, and are congruent with previous findings (Subbotin *et al.*, 2004, 2005; Chizhov *et al.*, 2010; Vovlas *et al.*, 2011; Oliveira *et al.*, 2013). Although *D. oncogenus* n. sp. showed an elevated similarity in D2–D3 and 18S with *D. gigas* and *D. dipsaci*, the ITS, *COI* and *hsp90* analyses showed enough resolution to distinguish among these species. Also, as previously demonstrated by Subbotin *et al.* (2005), there was certain congruence of the phylogeny of *Ditylenchus* spp. with their host plants. The phylogeny of ITS suggests that *Ditylenchus* might be a paraphyletic taxon including several evolutionary independent lineages, as was proposed previously by Oliveira *et al.* (2013).

Acknowledgements

The present work was supported with funds provided by the Italian Ministry of Economy and Finance to the National Research Council for the project 'Innovazione e Sviluppo del Mezzogiorno' – Conoscenze Integrate per Sostenibilità ed Innovazione del Made in Italy Agroalimentare – Legge n. 191/2009, and partially by grant AGR-136 from 'Consejería de Economía, Innvovación y Ciencia' from Junta de Andalucía and and Union Europea, Fondo Europeo de Desarrollo regional, 'Una manera de hacer Europa'.

Conflict of interest

None.

References

Abolafia, J., Liébanas, G. & Peña-Santiago, R. (2002) Nematodes of the order Rhabditida from Andalucia Oriental, Spain. The subgenus *Pseudacrobeles* Steiner, 1938, with description of a new species. *Journal of Nematode Morphology and Systematics* **4**, 137–154.

Boutsika, K., Brown, D.J.F., Phillips, M.S. & Blok, V.C. (2004) Molecular characterisation of the ribosomal DNA of *Paratrichodorus macrostylus, P. pachydermus, Trichodorus primitivus* and *T. similis* (Nematoda: Trichodoridae). *Nematology* **6**, 641–654.

Brzeski, M.W. (1991) Review of the genus *Ditylenchus* Filipjev, 1936 (Nematoda: Anguinidae). *Revue de Nématologie* **14**, 9–59.

Castillo, P., Vovlas, N., Subbotin, S. & Troccoli, A. (2003) A new root-knot nematode, *Meloidogyne baetica* n. sp. (Nematoda: Heteroderidae), parasitizing wild olive in Southern Spain. *Phytopathology* **93**, 1093–1102.

Chizhov, V.N., Borisov, B.A. & Subbotin, S.A. (2010) A new stem nematode, *Ditylenchus weischeri* sp. n. (Nematoda: Tylenchida), a parasite of *Cirsium arvense* (L.) Scop. in the central region of the Non-Chernozem zone of Russia. *Russian Journal of Nematology* **18**, 95–102.

Coolen, W.A. (1979) Methods for extraction of *Meloidogyne* spp. and other nematodes from roots and soil. pp. 317–329 *in* Lamberti, F. & Taylor, C.E. (*Eds*) *Root-knot nematodes (*Meloidogyne *species). Systematics, biology and control*. New York, Academic Press.

Darriba, D., Taboada, G.L., Doallo, R. & Posada, D. (2012) jModelTest 2: more models, new heuristics and parallel computing. *Nature Methods* **9**, 772.

Esser, R.P. (1986) A water agar *en face* view technique. *Proceedings of the Helminthological Society of Washington* **53**, 254–255.

Goodey, J.B., Franklin, M.T. & Hooper, D.J. (1965) *T. Goodey's The nematode parasites of plants catalogued under their hosts*. Farnham Royal, Bucks, England, Commonwealth Agricultural Bureaux.

Gulcu, B., Hazir, S., Gilbin-Davis, R.M., Ye, W., Kanzaki, N., Mergen, H., Keskin, N. & Thomas, W.K. (2008) Molecular variability of *Schistonchus caprifici* (Nematoda: Aphelenchoididae) from *Ficus carica* in Turkey. *Nematology* **10**, 639–649.

Hall, T.A. (1999) BioEdit: a user-friendly biological sequence alignment editor and analysis program for Windows 95/98NT. *Nucleic Acids Symposium Series* **41**, 95–98.

Hooper, D.J. (1986) Handling, fixing, staining and mounting nematodes. pp. 59–80 *in* Southey, J. (*Ed.*) *Laboratory methods for work with plant and soil nematodes*. 6th edn. London, Her Majesty's Stationery Office, Ministry of Agriculture, Fisheries and Food.

Huelsenbeck, J.P. & Ronquist, F. (2001) MRBAYES: Bayesian inference of phylogenetic trees. *Bioinformatics* **17**, 754–755.

Johansen, D.A. (1940) *Plant microtechnique*. New York, McGraw-Hill.

Karssen, G. & Willemsen, N.M. (2010) The spiculum: an additional useful character for the identification of *Ditylenchus dipsaci* and *D. destructor* (Nematoda: Anguinidae). *EPPO Bulletin* **40**, 211–212.

Oliveira, R.D.L., Santin, A.M., Seni, D.J., Dietrich, A., Salazar, L.A., Subbotin, S.A., Mundo-Ocampo, M., Goldenberg, R. & Barreto, R.W. (2013) *Ditylenchus gallaeformans* sp. n. (Tylenchida: Anguinidae) – a neotropical nematode with biocontrol potential against weedy Melastomataceae. *Nematology* **15**, 179–196.

Page, R.D. (1996) TreeView: an application to display phylogenetic trees on personal computers. *Computer Applications in the Biosciences* **12**, 357–358.

Siddiqi, M.R. (2000) *Tylenchida parasites of plants and insects*. 2nd edn. Wallingford, UK, CABI Publishing.

Skantar, A.M. & Carta, L.K. (2005) Phylogenetic evaluation of nucleotide and protein sequences from the heat shock protein 90 gene of selected nematodes. *Journal of Nematology* **36**, 466–480.

Sturhan, D. & Brzeski, M.W. (1991) Stem and bulb nematodes, *Ditylenchus* spp. pp. 423–464 *in* Nickle, W.R. (*Ed.*) *Manual of agricultural nematology*. New York, Marcel Dekker.

Subbotin, S.A. & Moens, M. (2006) Molecular taxonomy and phylogeny. pp. 33–58 *in* Perry, R. & Moens, M. (*Eds*) *Plant nematology*. Wallingford, UK, CABI.

Subbotin, S.A., Vierstraete, A., De Ley, P., Rowe, J., Waeyenberge, L., Moens, M. & Vanfleteren, J.R. (2001) Phylogenetic relationships within the cyst-forming nematodes (Nematoda, Heteroderidae) based on analysis of sequences from the ITS regions of ribosomal DNA. *Molecular Phylogenetics and Evolution* **21**, 1–6.

Subbotin, S.A., Krall, E.L., Riley, I.T., Chizhov, V.N., Staelens, A., De Loose, M. & Moens, M. (2004) Evolution of the gall-forming plant parasitic nematodes (Tylenchida: Anguinidae) and their relationships with hosts as inferred from Internal Transcribed Spacer sequences of nuclear ribosomal DNA. *Molecular Phylogenetics and Evolution* **30**, 226–235.

Subbotin, S.A., Madani, M., Krall, E., Sturhan, D. & Moens, M. (2005) Molecular diagnostics, taxonomy, and phylogeny of the stem nematode *Ditylenchus dipsaci* species complex based on the sequences of the internal transcribed spacer-rDNA. *Phytopathology* **95**, 1308–1315.

Swofford, D.L. (2003) PAUP*: Phylogenetic Analysis Using Parsimony (and other methods). 4.0 Beta. Florida State University.

Teploukhova, T.N. (1968) Stem and bulb nematodes (genus *Ditylenchus* Filipjevi, 1936: family Tylenchidae Örley, 1880) of fauna of USSR and neighbour countries. PhD Thesis, Zoological Institute of the Academy of Science of USSR (in Russian).

Thompson, J.D., Higgins, D.G. & Gibson, T.J. (1994) Clustal W: improving the sensitivity of progressive multiple sequence alignment through sequence weighting, positions-specific gap penalties and weight matrix choice. *Nucleic Acids Research* **22**, 4673–4680.

Thorne, G. (1945) *Ditylenchus destructor* n. sp., the potato root nematode and *D. dipsaci* (Kühn, 1857), Filipjev, 1936, the teasel nematode. *Proceedings of the Helminthological Society of Washington* **12**, 27–33.

Troccoli, A. (2002) Aspetti pratici e comparativi di alcune metodologie tradizionali applicate all'identificazione dei nematodi da quarantena. *Nematologia Mediterranea* **30**, 107–110.

Vovlas, N., Troccoli, A., Palomares-Rius, J.E., De Luca, F., Liébanas, G., Landa, B.B., Subbotin, S.A. & Castillo, P. (2011) *Ditylenchus gigas* n. sp. parasitizing broad bean: a new stem nematode singled out from the *Ditylenchus dipsaci* species complex using a polyphasic approach with molecular phylogeny. *Plant Pathology* **60**, 762–775.

Zhang, S.L., Liu, G.K., Janssen, T., Zhang, S.S., Xiao, S., Li, S.T., Couvreur, M. & Bert, W. (2014) A new stem nematode associated with peanut pod rot in China: morphological and molecular characterization of *Ditylenchus arachis* n. sp. (Nematoda: Anguinidae). *Plant Pathology* **63**, 1193–1206.